

MODELLING, IDENTIFICATION AND PERFORMANCE ANALYSIS OF A GLASS FIBRE BUSHING

J. Brély^{*,**} O. Sename^{**} L. Dugard^{**} N. Marsault^{*}

** Saint-Gobain Vetrotex International, 767 Quai des Allobroges -
BP 929, 73009 Chambéry, FRANCE
Fax : 33 (0)4.79 75 53 24
email : {julien.brely,nicolas.marsault}@saint-gobain.com*

*** Laboratoire d'Automatique de Grenoble, ENSIEG-BP 46,
38402 Saint Martin d'Hères Cedex, FRANCE
Fax : 33 (0)4.76.82.63.88
email : {olivier.sename,luc.dugard}@inpg.fr*

Abstract: This paper is devoted to the identification and control of a glass fibre bushing. First a mathematical model, based on physical equations (electric, hydraulic and thermal balances), allows to predict the throughput, the electric power consumed and the temperature of the tip plate of the bushing. Then controls oriented linear models are obtained via experimental identification on the industrial process. Performance analysis of the existing control system is then provided by identifying the usual sensitivity functions on real data.

Keywords: glass fibre, modelling, identification, sensitivity functions, performance analysis

1. INTRODUCTION

This work concerns the regulation of a glass fibre bushing. Indeed, today, the products quality and the production yields are not completely satisfactory. Moreover, very simple, and not "optimal", control strategies of bushing, such as PI controllers, are used currently in Vetrotex plants. The industrial challenge is then to provide a methodology for designing a control system, ensuring good production indicators, in the considered industrial framework. In this paper, the bases of control system design are tackled, i.e. the modelling of the process using identification algorithms, and the way to quantify the performances of the control system using the well-known sensitivity functions. As the glass fibre production works in closed-loop, experimental identification procedures will be done in closed-loop. The collected real data are then used to perform identification algorithms. Furthermore, the existing controller will be analyzed, allowing future improvement of the control strategies. Another important aim is to put in place tools which will be used for multi-variable (i.e. multi types of glass fibre) control

system design.

This paper is organized as follows. In Section 2 the industrial process is presented. A mathematical model is described in Section 3. In Section 4 the identification procedure is explained. The bushing transfer function is identified in Section 5. In Section 6 performances of the control system are analyzed. Conclusions are given in Section 7.

2. THE PROCESS

Glass is a phase we exceptionally find in nature and always after a sudden cooling of melted rocks. Glass is often a brittleness symbol. However, when glass is fibered under the form of fine filaments and when these filaments are collected in strands to do glass fibre, its resistance is higher than best steels resistance. Moreover, glass fibre is an excellent electric isolant, is non-flammable and has a very low sensitivity to thermal variations. Glass fibre is very used for the reinforcement of organic and mineral matrices, to do what it is called "composites". Glass fibre is particularly useful in three main domains:

- in electronic, such as to produce copper-plated laminates in printed circuit board manufacture.
- in building, where glass fibre is incorporated in cement matrix.
- in automotive, where it is used in body panels.

2.1 The Glass Fibre Production

Here is a short presentation of the glass fibre production. For more details see [Loewenstein, 1993]. The fabrication steps are the following ones: raw materials for glass fabrication are heated in a furnace at a temperature of 1400°C . At a such temperature, the glass is fluid. Then it flows by gravity down shafts in refractory material up to the bushing, a parallelepiped box jailed in cement. The upper part of a bushing, called the screen, is a pierced plate, heated by Joule effect. Its goal is to homogenize glass temperature around 1250°C in order to compensate heat losses during its transport. The lower part (the tip plate) is a pierced plate with tips. The figure 1 represents the different parts of a bushing.

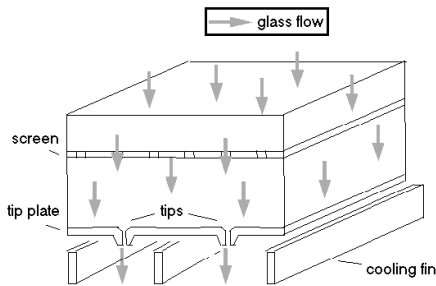


Fig. 1. Scheme of a bushing

The tip plate is in contact with air. Glass flows down the tips by gravity and glass threads are mechanically drawn by winders to form filaments, with a diameter varying from 5 to $24\mu\text{m}$. A chemical product, called the size, is added at this moment to the filaments in order to confer good mechanical and antistatic properties to the filaments which are linked together to form glass fibre. The figure 2 is a simplified representation of the fabrication process.

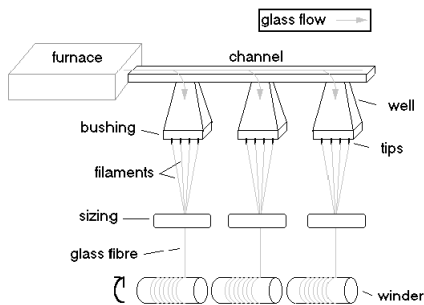


Fig. 2. Scheme of a glass fibre production process

A glass fibre is generally characterized by its linear weight (g/km) and a bushing by its tips number and its throughput (kg/day).

2.2 The Regulation

As throughput can not be measured, only the bushing temperature which is linked to the throughput, is measured and controlled.

Bushing temperature control plays an essential role in the quality of the produced glass fibre. The purpose of a stable temperature is two-fold. As glass throughput strongly depends on bushing temperature, a stable temperature avoids the variations of fibres diameter. Moreover, by avoiding strong variations of glass throughput, a stable temperature causes less production breaks.

The regulation loop (see figure 3) is made by a controller, actuators and a bushing. Actuators are a thyristor block and a transformer. The control input is, via the thyristor block opening, the electric power supplied to the bushing. The feedback data is the temperature of the bushing. Today the control strategy is an industrial PID, including some additional filters.

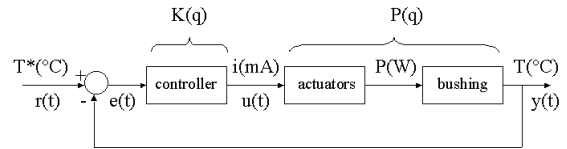


Fig. 3. Scheme of a glass fibre production process

In the next part the mathematical model of a glass fibre bushing is developed.

3. MATHEMATICAL MODEL BASED ON PHYSICAL KNOWLEDGE

Vetrotex uses complex models for bushing simulation and design, but they are useless for the real-time control. The mathematical model relies on many different physic domains, as electric, hydraulic and thermal. The physical laws on which the model is based are detailed. The figure 4 is a scheme of the model.

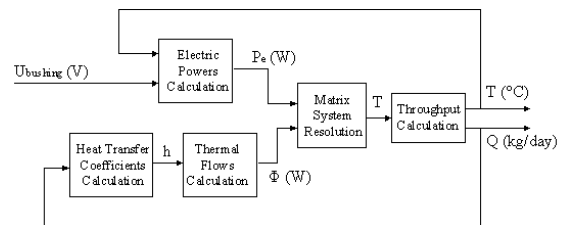


Fig. 4. Scheme of a bushing model

3.1 Electric Equations

Using the bushing geometry and the electric conductivity σ ($\Omega^{-1}.\text{m}^{-1}$) depending of the temperature T ($^{\circ}\text{C}$) of the components of the bushing, the electric

resistance of all the plates composing the bushing is given by:

$$R(T) = \frac{L}{\sigma(T) \cdot S} \quad (1)$$

where L is the length (m) and S the section (m^2) of the plate.

The electric power P_e (W) lost by Joule effect in all the components of the bushing is:

$$P_e(T) = \frac{U^2}{R(T)} \quad (2)$$

where U (V) is the voltage between the terminals of the bushing.

3.2 Thermal Balances

The thermal energy of an object is given by

$$E = m \cdot c_p \cdot T \quad (3)$$

where m is the mass (kg) and c_p the heat capacity ($J.K^{-1}.kg^{-1}$) of the object.

For a pierced plate, the variation of thermal energy ΔE per time unit is equal to

$$\frac{\Delta E}{\Delta t} = m \cdot c_p \cdot \frac{\Delta T}{\Delta t} = P_e + \phi_{in} - \phi_{out} \quad (4)$$

where P_e represents the electric power source, ϕ_{in} the glass inflow, ϕ_{out} the glass outflow.

To determine the temperature in the bushing, we need to know all energy flows. Glass flows ϕ_{in} and ϕ_{out} are characterized by the three types of heat transfers, which are:

- Conduction. The flow ϕ_{cond} is given by the Fourier's law:

$$\phi_{cond} = \lambda \cdot S_1 \cdot \frac{dT}{dx} = \lambda \cdot S_1 \cdot \frac{\Delta T}{\Delta x} \quad (5)$$

where λ is the thermal conductivity ($W.m^{-1}.K^{-1}$) and S_1 the contact area (m^2).

- Convection. The flow is expressed by the following relation:

$$\phi_{conv} = h \cdot S_2 \cdot \Delta T \quad (6)$$

where h is the coefficient of convection ($W.m^{-2}.K^{-1}$) and S_2 the contact area (m^2).

- Radiation. The radiative flow is obtained by the relation:

$$\phi_{rad} = \epsilon \cdot \sigma \cdot S_3 \cdot (T^4 - T_0^4) \quad (7)$$

where ϵ is the emissivity of the object, S_3 the contact area (m^2) and σ the Stefan-Boltzmann constant. ($\sigma = 5.67.10^{-8} W.m^{-2}.K^{-4}$)

3.3 The Hydraulic Equation

The temperatures of the screen and of the tip plate allow to calculate the glass viscosity (μ , in Poises) at the screen and at the tip plate, as:

$$\log(\mu(T)) = A + \frac{B}{T - T_0} \quad (8)$$

where A , B et T_0 are real constants depending on the type of glass.

The bushing throughput Q ($kg.s^{-1}$) is thus given by the following equation:

$$Q = \frac{\rho^2 \cdot g \cdot H}{R_s \cdot \mu(T_s) + R_p \cdot \mu(T_p)} \quad (9)$$

where ρ is the glass density ($kg.m^{-3}$), g the gravity constant ($m.s^{-2}$), H the glass height (m) from the tip plate, and R_s and R_p are the geometric resistances (m^{-3}) of the screen and of the tip plate.

Physical equations are nonlinear but, around the operating point, the model can be considered as linear. This assumption will be used in the identification procedure, where linear models will be obtained.

4. BACKGROUNDS ON CLOSED LOOP IDENTIFICATION

The practical importance of plant model identification has been recognized for many years. In our industrial framework, the temperature variations in open loop can disrupt the production, which is not satisfactory. Closed-loop identification is performed around a glass temperature set-point.

4.1 The Identification Process

System identification allows to get a model that describes the dynamical behavior of the process. The obtained model is valid only around the set-point (few C). The identification process is described in [Ljung, 1987].

The initial step is to obtain good experimental data. To realize a good identification the reference input sequence should be as informative as possible, i.e. have a strong frequency content in interesting frequency ranges. A *pseudo random binary sequence* (PRBS) is then chosen. The second step is the selection of a model structure. Among the classical ones (ARX, ARMAX, OE, ...), an ARMAX structure is chosen and represented under the following form:

$$A(q)y(t) = q^{-d}B(q)u(t) + C(q)e(t) \quad (10)$$

with:

- $A(q) = 1 + a_1 \cdot q^{-1} + \dots + a_{n_A} \cdot q^{-n_A}$
- $B(q) = b_1 \cdot q^{-1} + \dots + b_{n_B} \cdot q^{-n_B}$
- $C(q) = 1 + c_1 \cdot q^{-1} + \dots + c_{n_C} \cdot q^{-n_C}$

where $y(t)$ is the output signal, $u(t)$ the input signal, $e(t)$ a white noise and q the shift operator. Such a

model is noted $[n_A \ n_B-1 \ n_C \ d]$ in what follows. The following step is the choice of a criterion which will give informations on how well the model fits the experimental data. We use a very usual criterion: the *final prediction error* (FPE). The fourth step is the parameter estimation and allows to determinate the coefficients of the chosen structure. The last step consists in validating the model thanks to tools such as step response, Bode diagram, poles and zeros, model residuals,...

4.2 Three Stage Identification

Among the closed-loop identification methods described in the literature as in [Karimi and Landau, 1998], the three stage procedure is here used (see [Ebert et al., 1997]). It needs output signal $y(t)$, reference input signal $r(t)$ and command signal $u(t)$ (output of the controller). This method does not require the knowledge of the controller transfer function. The principle is the following one:

- Determine the complementary sensitivity function T from $y(t)$ and $r(t)$ and the sensitivity function on the input KS from $u(t)$ and $r(t)$.
- Reconstruct the signals $y_r(t)$ and $u_r(t)$ with $r(t)$ and respectively T and KS .
- Identify the model from $y_r(t)$ and $u_r(t)$.

This model is then compared with the one given by a direct identification method between the signals $y(t)$ and $u(t)$.

5. IDENTIFICATION OF THE BUSHING TRANSFER FUNCTION

In [Åström and Wittenmark, 1997] it is advised to take a sampling period T_e such as:

$$\frac{T_r}{T_e} = 4 \text{ to } 10 \quad (11)$$

where T_r is the rise time of the system. So a value of 5s for T_e represents a good choice in our case.

A time base of 20s and a magnitude of 1°C for the PRBS are taken to have a good excitation of the process dynamic. This PRBS is given as reference input signal in the controller. Data are collected in the form of $4 - 20\text{mA}$ signals, using industrial data acquisition modules.

5.1 Direct Identification of the Bushing Transfer Function

The transfer function of the bushing $P(q)$ is the transfer function between the output signal $y(t)$ and the command signal $u(t)$.

The "best" found ARMAX model is $[2 \ 2 \ 1 \ 1]$, the criterion is $FPE(P) = 4.6 * 10^{-2}$ and the transfer function is:

$$P(q) = \frac{0.53(q - 0.66)}{(q - 0.92)(q - 0.05)} \quad (12)$$

5.2 Identification of the Bushing Transfer Function by the Three Stage Method

As mentioned previously, this method needs to identify two sensitivity functions. Both identifications are described in the next section devoted to performance analysis. So, in this part, we consider only the results of the three stage method. The obtained ARMAX model is $[5 \ 5 \ 1 \ 1]$ and $FPE(P) = 7.3 * 10^{-2}$.

The figure 5 represents the Bode diagrams of $P(q)$ corresponding to both identification methods.

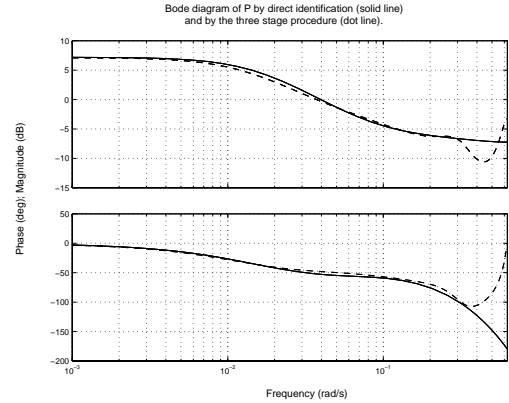


Fig. 5. Identification results

It is important to notice that both model diagrams coincide except in high frequency where the model orders difference appears. Indeed, high frequency dynamics are difficult to identify.

5.3 Validation through the sensitivity functions

A criterion to estimate the quality of the identification of $P(q)$ by the direct method is the comparison of Bode diagrams of $T(q)$ obtained by identification and of $\frac{P(q).K(q)}{1+P(q).K(q)}$ reconstructed via the identifications of $P(q)$ and $K(q)$.

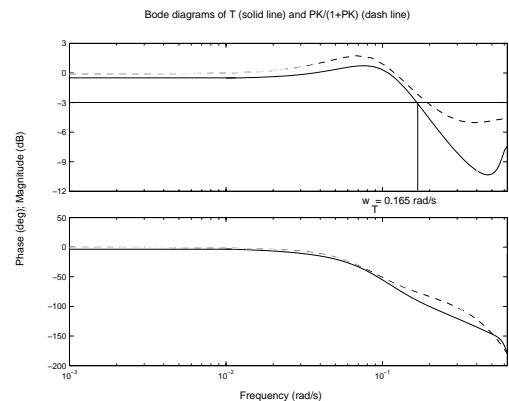


Fig. 6. $T(q)$: Zeroes = $(0.59, -0.59)$ Poles = $(0.66 + 0.27i, 0.66 - 0.27i, -0.73)$

$T(q)$ is an ARMAX model $[3 \ 3 \ 2 \ 1]$ where $FPE(T) = 6.9 * 10^{-3}$. $K(q)$ is a controller represented by an ARMAX model $[1 \ 2 \ 1 \ 0]$ where $FPE(K) = 1.3 * 10^{-3}$. Except at high frequency,

both Bode diagrams coincide, this validates the identification of $P(q)$ by the direct method. At low frequency, the value of the gain is $-0.50dB$. This gain, close to $0dB$, means that there is a very low steady-state error.

These preliminary results, even incomplete, show that the second order model for $P(q)$ is convenient. Moreover, experimental time domain validation has been performed using different sets of input data. In the next section, we study the performances of the existing closed-loop system.

6. PERFORMANCE ANALYSIS

In this part the usual tools for performance analysis, i.e. the sensitivity functions, are identified and analyzed. The aim of the performance analysis is to study how the reference is tracked and how disturbances and noises are rejected.

6.1 Criteria for the Performance Analysis

The more useful tools to discuss about control system performances are derived through the sensitivity functions. The sensitivity functions are transfer functions between variables of the control system.

The three sensitivity functions are (see Figure 3):

- The sensitivity function $S(q)$ is the transfer function between the control error $e(t)$ and the reference input sequence $r(t)$.
- For $T(q)$ and $KS(q)$, see section 4.2.

Moreover, let us introduce the open loop transfer function $L(q)$, which is the transfer function between the output signal $y(t)$ and the error $e(t)$.

6.1.1. Phase and Gain Margins Noted Δ_ϕ and Δ_G , the phase and gain margins describe the robustness in stability of the control system:

$$\Delta_\phi = 180 + \arg(L(j\omega_c)) \quad \text{where } |L(j\omega_c)| = 0dB$$

$$\Delta_G = \frac{1}{|L(j\omega_{180})|} \quad \text{where } \arg(L(j\omega_{180})) = -180^\circ$$

As pointed in [Goodwin et al., 2001], "the phase margin quantifies the pure phase delay that should be added to achieve the same critical condition, and the gain margin indicates the additional gain that would take the closed loop to the critical stability condition". It is often required to have $\Delta_\phi > 30^\circ$ and $\Delta_G > 6dB$. The phase and gain margins are used to provide the appropriate trade-off between performance and stability.

6.1.2. Module Margin Δ_M It is a robustness criterion. The module margin is characterized for the SISO systems as the inverse of the largest value of $|S(j\omega)|$, noted M_S . It represents the minimal distance from the Nyquist curve to the critical point -1 . So, to have good robustness, the module margin must not be too low, typically $\Delta_M \geq 0.5$.

6.1.3. Frequency Domain Peaks The maximum peaks (M_S and M_T) of the sensitivity and complementary sensitivity functions are robustness indicators. Indeed, the smaller M_S is, the better the robustness is. Skogestad and Postlethwaite [1996] advise to impose $M_S < 6dB$ and $M_T < 2dB$. Moreover the maximum of $|KS(j\omega)|$ is related to the actuator constraint.

6.1.4. Bandwidth In [Skogestad and Postlethwaite, 1996] the bandwidth frequency is defined as the frequency ω_S where $|S(j\omega)|$ crosses at first $-3dB$ from below. This frequency characterizes the performances of the control system. Indeed, for frequencies smaller than the bandwidth frequency, the output disturbances effects on the controlled output will be rejected. Bandwidth may also be defined for the remaining sensitivity functions. For example, the bandwidth frequency ω_T of $|T(j\omega)|$ characterizes the tracking of the closed-loop system. Nevertheless we should have $\omega_S < \omega_c < \omega_T$. In [Skogestad and Postlethwaite, 1996] the rise time t_r of the closed-loop system is approximated by the relation:

$$t_r \simeq \frac{2.3}{\omega_T} \quad (13)$$

All the definitions characterize the input/output performances of the control system.

6.2 Performance Analysis

In this part direct identification methods are used.

6.2.1. Output Performance Analysis The output performances are characterized by analysing the characteristics of $L(q)$, $S(q)$ and $T(q)$, obtained by identification.

- Identification of $L(q)$: the ARMAX model chosen for $L(q)$ is $[3 \ 4 \ 2 \ 1]$. The value of the identification criterion is $FPE(L) = 2.5 * 10^{-3}$.

The figure 7 represents the Nichols charts of $L(q)$.

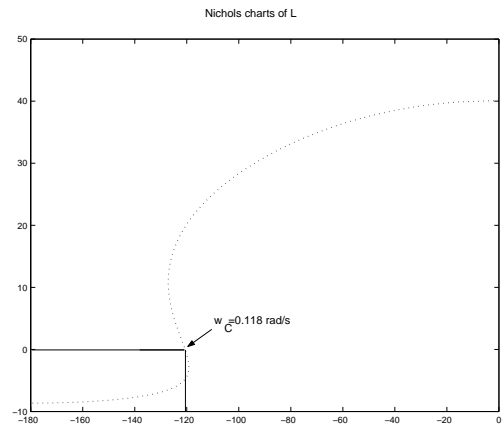


Fig. 7. $L(q)$: Zeroes = $(0.66, \ 0.28)$
Poles = $(0.98, \ 0.92, \ 0.05)$

The phase margin value is 59° . The corresponding frequency is $\omega_c = 0.118\text{rad/s}$. The gain margin value is 8.7dB . As it is required to have $\Delta_\phi > 30^\circ$ and $\Delta_G > 6\text{dB}$, the system has good stability margins.

- Identification of $S(q)$: the ARMAX model chosen for $S(q)$ is $[3 \ 4 \ 1 \ 0]$. The value of the criterion is $FPE(S) = 9.7 * 10^{-3}$.

The figure 8 represents the Bode diagram of $S(q)$.

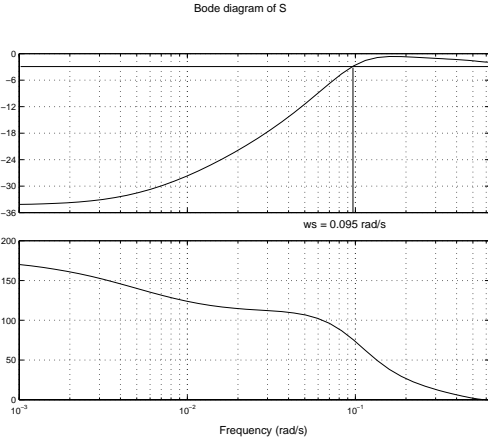


Fig. 8. $S(q)$: Zeroes = $(1.03, 0.78, -0.46)$
Poles = $(0.66 + 0.31i, 0.66 - 0.31i, -0.42)$

The maximum M_S of the gain curve is 0.64dB , so the value of the module margin is 1.56. As $\Delta_M \geq 0.5$, it ensures good robustness properties. Moreover the curve crosses first -3dB for $\omega_S = 0.095\text{rad/s}$. So the output disturbances are rejected for $\omega < \omega_S$.

- Identification of $T(q)$ (see figure 6): we have obtained $M_T = 0.50\text{dB}$. As $M_T < 2\text{dB}$, it proves that robustness properties are satisfactory. The Bode diagram of $T(q)$ crosses first -3dB for $\omega_T = 0.165\text{rad/s}$. So the inequality $\omega_S < \omega_c < \omega_T$ is satisfied. Moreover, according to the relation (13), the rise time of the closed-loop system should be 14s. Experimentally the found rise time is 13s, which confirms the identifications.

6.2.2. Input Performance Analysis The input performances are linked to the characteristics of $KS(q)$. So the identification of $KS(q)$ is needed. The chosen ARMAX model for $KS(q)$ is $[3 \ 4 \ 1 \ 0]$. The value of the criterion is $FPE(KS) = 1.5 * 10^{-2}$. The figure 9 shows the Bode diagram of $KS(q)$.

The gain curve crosses -3dB from above for $\omega_{KS} = 0.615\text{rad/s}$. So measurement noises may affect the actuators.

Note that all the sensitivity functions should have the same poles. Among the three poles, only complex poles are common to all the sensitivity functions. This difference can be explained by the fact that there are additional filters inside the controller.

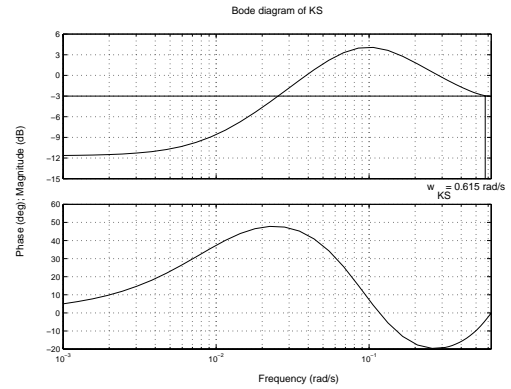


Fig. 9. $KS(q)$: Zeroes = $(0.95, 0.15, -0.18)$
Poles = $(0.65 + 0.18i, 0.66 - 0.18i, -0.11)$

7. CONCLUSION

A second order model has been identified and validated, and a performance analysis has been provided using the sensitivity functions. The control system performances are satisfactory, but they can be improved, particularly for the sensitivity of the control (actuators) to the measurement noises. A comparative study will be made with advanced control (LQ, H2,...). Moreover such a methodology, based on the sensitivity functions, may also be used for MIMO systems such as multi-products bushing. Comparison of the real time simulation of the physical model with the identified model and experimental data will be performed and MIMO control will be developed in the future.

References

- K.J. Åström and B. Wittenmark. *Computer Controlled System: Theory and Design*. Prentice-Hall, 1997.
- W. Ebert, M. M'Saad, and J. Chebassier. Three stage procedure for closed loop identification. In *Proc. of the European Control Conference 97*, Brussels, Belgium, 1997.
- G.C. Goodwin, S.F. Graebe, and M.E. Salgado. *Control System Design*. Prentice-Hall, 2001.
- A. Karimi and I.D. Landau. Comparison of the closed loop identification methods in terms of bias distribution. *Systems and Control Letters*, 34(4): 159–167, 1998.
- L. Ljung. *System Identification: Theory for the User*. Prentice-Hall, 1987.
- K.L. Loewenstein. *The Manufacturing Technology of Continuous Glass Fibres*. Elsevier Science Publishers, 1993.
- S. Skogestad and I. Postlethwaite. *Multivariable Feedback Control: Analysis and Design*. John Wiley & Sons, 1996.